ChemComm

Accepted Manuscript

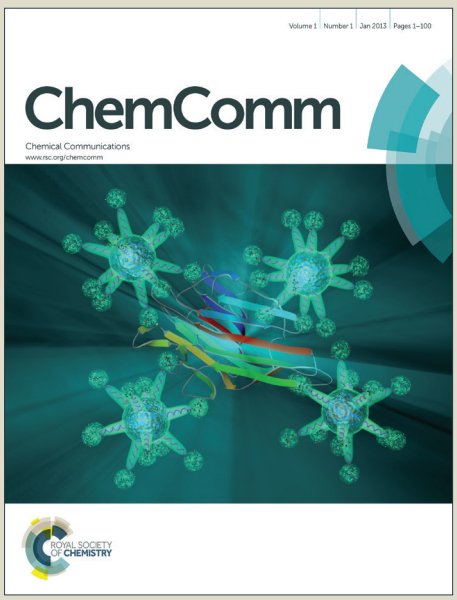

ROYAL SOCIETY OF CHEMISTRY

www.rsc.org/chemcomm

Ultrafast cation intercalation in nanoporous nickel hexacyanoferrate

Takayuki Shibata[a] **and Yutaka Moritomo***[a,b]

Received Xth XXXXXXXXXX 20XX, Accepted Xth XXXXXXXXX 20XX
First published on the web Xth XXXXXXXXXX 200X
DOI: 10.1039/b000000x

Cation intercalation into nanoporous coordination polymer is utilized in, *e.g*, Li^+/Na^+ secondary battery, decontamination of radioactive $^{137}Cs^+$, and so on. Here, we observed an ultrafast intercalation of Na^+ and Rb^+ within 1500 ms in a thin film of nickel hexacyanoferrate, $Na_{0.68}Ni[Fe(CN)_6]_{0.67}5.0H_2O$, in aqueous solutions. Quantitative analyses of the intercalation kinetics revealed that the high cation diffusion constant ($D \sim 10^{-9}$cm^2/s) is responsible for the intercalation.

Coordination polymer consists of metal and ligand unit, and forms one-, two-, or three-dimensional metal - ligand network. The resultant periodic nanospaces cause useful functionalities. For example, the nanospaces can reversibly store the neutral molecules, *e.g.*, H_2, N_2, O_2, CO_2, and H_2O, by an external gas-pressure.[1,2] If the valence of the constituent metal and/or ligand is controllable, the nanospaces can store the cations,[3–27] *e.g.* Li^+, Na^+, K^+, Rb^+, Cs^+, Ca^{2+}, Mg^{2+}, Sr^{2+} and Ba^{2+}. In this case, an external voltage reversibly controls the intercalation/deintercalation of the cation via the reduction/oxidization process of the host framework.

Among the coordination polymers, Prussian blue (PB) and its analogues (PBA) are intensively investigated from a viewpoint of electrochemistry.[3–12] PBA, represented as $A_xM[Fe(CN)_6]_yzH_2O$ (A and M are alkali and transition metal, respectively), forms a three-dimensional (3D) jungle-gym-type network, which causes cubic nanospace of 5 Å at the edge.[28,29] A thin film of PB, $Fe^{III}[Fe^{II}(CN)_6]_{3/4}$, exhibits a reversible blue-transparent electrochromism,[3,4] reflecting the reduction process of Fe^{III}. The mixed-valence state of PB was thermodynamically analyzed with a solid solution model of PB and Everitt's salt (ES).[11,12] However, the redox process of PB is rather complicated: several electrogravimetry investigations[5,7] suggest considerable contribution of H^+ in addition to A^+. This makes a sharp contrast with the case of nickel hexacyanoferrate[8] and cobalt hexacyanoferrate[9,10], in which only A^+ takes part in the redox process.

Recentry, the ion storage functionality of PBA gathers increasing attention of material scientists,[13–27] because they can store Li^+ and Na^+ in aprotic solvent and can be utilized as a cathode material for Li^+ (Na^+) secondary battery. For example, a thin film of manganese hexacyanoferrate[17,18] exhibits a capacity of 128 (109) mAh/g and an average voltage of 3.8 (3.4) V vs. Li (Na) in the Li^+ (Na^+) secondary battery. In addition, PBA can store divalent alkaline-earth metal ion[15,27] as well as larger alkali metal ion.[30,31] These storage functionalities can be utilized for removal/condensation of specific cation, *e.g.*, removal of radioactive $^{137}Cs^+$ from aqueous solution. In general, electrochemical kinetic of the electrode reaction in the solvent (electrolyte) - solid (material) system is described by the diffusion equations in the both regions with the boundary condition of Butler-Volmer equation.[32] However, this model is too complicated with many adjustable parameters to be applied to the actual intercalation kinetics. A more simple and intuitive model is indispensable to comprehend the cation diffusion effect in solid on the intercalation kinetics in a wide range of nanoporous materials.

In this Communication, we reported a fast intercalation of Na^+ and Rb^+ in thin film of nickel hexacyanoferrate, $Na_{0.68}Ni[Fe(CN)_6]_{0.67}5.0H_2O$ (abbreviated as NNF67). The intercalation kinetics was analyzed by a phenomenological model with a time-independent cation transfer rate (α) at the solvent/solid interface. We ascribed the fast cation intercalation to high cation diffusion constant (D) of NNF67: D = 0.9×10^{-9}cm^2/s for Na^+ and 0.7×10^{-9}cm^2/s for Rb^+.

The NNF67 film was electrochemically synthesized on an indium tin oxide (ITO) transparent electrode under potentiostatic conditions at 0.40 V vs. a standard Ag/AgCl electrode in an aqueous solution containing 0.5mM $K_3[Fe^{III}(CN)_6]$, 0.5mM $Ni^{II}(NO_3)_2$, and 1.0M $NaNO_3$.[8] The obtained film was transparent with a thickness of 500 - 600 nm. Chemical composition was determined using the inductively coupled plasma (ICP) method and a CHN organic elementary analyzer. Calcd: Na, 5.2; Ni, 18.3; Fe, 12.3; C, 15.9; H, 3.3; N, 18.6%. Found: Na, 6.2; Ni, 18.4; Fe, 12.5; C, 15.6; H, 3.3; N, 17.7%. For comparison, we synthesized a thin film of $Na_{1.52}Co[Fe(CN)_6]_{0.88}3.1H_2O$ (NCF88) in an aqueous solution containing 0.8mM $K_3[Fe^{III}(CN)_6]$, 0.5mM $Co^{II}(NO_3)_2$, and 5.0M $NaNO_3$.[10] The obtained film was transparent green with a thickness of 600 nm. Chemical composition was de-

[a] *Division of Physics, University of Tsukuba, Tennodai 1-1-1, Tsukuba, Ibaraki 305-7571, Japan. E-mail: moritomo.yutaka.gf@u.tsukba.ac.jp*
[b] *Tsukuba Research Center for Interdisciplinary Materials Science (TIMS), University of Tsukuba, Tsukuba, Ibaraki 305-8571, Japan*

termined using the ICP method and a CHN organic elementary analyzer. Calcd: Na, 10.4; Co, 17.6; Fe, 14,6; C, 18.9; H, 1.8; N, 22.0%. Found: Na, 11.2; Co, 17.4; Fe, 15.3; C, 18.5; H, 1.9; N, 20.0%. The XRD pattern of the NNF67 and NCF88 films can be indexed with the face-centered cubic setting (see Fig. S1). The NNF67 film shows flat surface, while the NCF88 film consists of small crystals (Fig. S2).

The cation intercalation kinetics was investigated with a beaker-type three-electrode cell. The working, referential, and counter electrodes were the PBA film, a standard Ag/AgCl electrode, and Pt, respectively. The electrolytes were aqueous solutions of NaCl and RbCl. First, the film was slowly oxidized under a constant current condition (= 10 μA/cm^2) with a cut-off voltage of 1.0 V. In this oxidation process, $Na_{0.68}Ni^{II}[Fe^{II}(CN)_6]_{0.67} \rightarrow 0.67e^- + 0.67Na^+ + Na_{0.01}Ni^{II}[Fe^{III}(CN)_6]_{0.67}$, the film color changes from transparent to yellow. We confirmed that the reduction of the cation density (x) is equal to the reduction charge (Fig. S3). The variation of the Fe valence was confirmed by the IR spectroscopy (Fig. S4). The intercalation kinetics was monitored by the current density (I) against time (t) under a constant external voltage (V_{ex}).

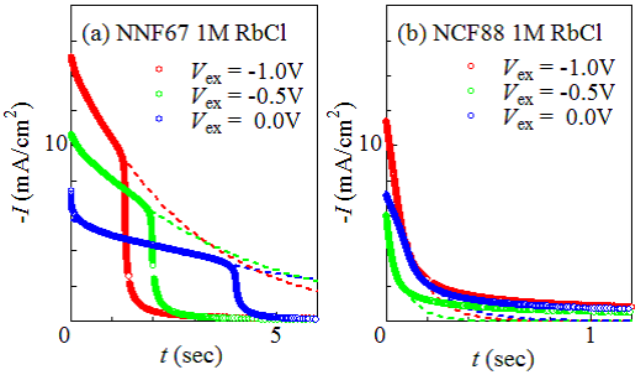

Fig. 1: Current density (I) of (a) NNF67 and (b) NCF88 in an aqueous solution of 1M RbCl under external voltage (V_{ex}) against time (t). Broken curves are results of the least-squares fitting with an exponential function, $I = I_0 \cdot \exp(-t/\tau)$.

As prototypical example, we show in Fig. 1(a) the I - t curves of the NNF67 film in an aqueous solution of 1M RbCl. At V_{ex} = - 1.0 V, the magnitude of I gradually decreases with t, and suddenly drops to zero at t = 1300 ms. We observed a concomitant color change from yellow to transparent (Fig. S5). The negative current indicates fast intercalation of Rb^+ into the film, $0.67e^- + 0.67Rb^+ + Na_{0.01}Ni^{II}[Fe^{III}(CN)_6]_{0.67} \rightarrow Rb_{0.67}Na_{0.01}Ni^{II}[Fe^{II}(CN)_6]_{0.67}$. A similar fast intercalation is observed in an aqueous solution of 1M NaCl: I suddenly drops to zero at t = 1500 ms at V_{ex} = - 1.0 V (Fig. S6). The discontinuous drop of - I is ascribed to completion of the cation intercalation. Actually, the intercalated cation densities (Δx) are close to the ideal value (0.67 per Ni): Δx = 0.80, 0.74, and 0.76 per Ni at V_{ex} = - 1.0, - 0.5, and 0.0 V, respectively. On the other hand, the gradual decrease of - I is well reproduced by an exponential function: $I = I_0 \cdot \exp(-t/\tau)$, where I_0 and τ are the initial current density and the relaxation time, respectively [broken curves in Fig. 1(a)]. Figure 2 shows (a) I_0 and (b) τ against V_s - V_{ex}, where V_s (= 0.4 V for NaCl and 0.7 V for RbCl) is the self-potential. $|I_0|$ linearly increases with V_s - V_{ex}, while the τ value slightly decreases as V_s - V_{ex} increases. Crosses in Fig, 2 are the parameters of $Na_{1.48}Ni[Fe(CN)_6]_{0.87}5.5H_2O$ powder (see Fig. S7).

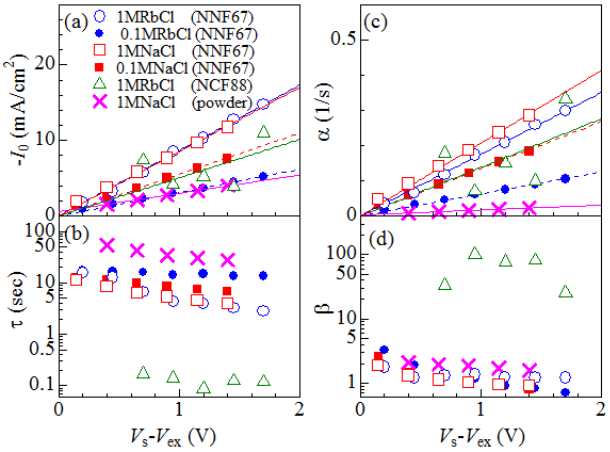

Fig. 2: (a) Initial current density (I_0), (b) relaxation time (τ), (c) cation transfer rate (α), and (d) surface coefficient (β) against V_s - V_{ex}, where V_s and V_{ex} is the self-potential and external voltage, respectively. Straight lines in (a) and (c) are results of the least-squares fitting.

The high-I value [Fig. 1(a)] indicates that the cation quickly diffuses into the inner side of the solid before the subsequent cation transfer. Actually, the cation diffusion constant (D) is significantly high in NNF67: $D = 0.9\times10^{-9}$cm^2/s for Na^+ and 0.7×10^{-9}cm^2/s for Rb^+ (Fig. S8). In this situation, *i.e.*, when the cation transfer from solvent is slower than the diffusion in solid, the intercalation kinetics is limited by the cation transfer [Fig. 3(a)]. In the opposite case, *i.e.*, when the diffusion is slower than the transfer, the kinetics is limited by the cation diffusion [Fig. 3(b)]. We investigated the kinetics of the Rb^+ intercalation in the NCF88 film [Fig. 1(b)], whose D is much lower than that of the NNF67 film (Fig. S9). Reflecting the residual surface cations, Δx is far below the ideal value (= 0.88 per Co): Δx = 0.02, 0.01, and 0.02 per Co at V_{ex} = - 1.0, - 0.5, and 0.0 V, respectively.

Finally, let us phenomenologically analyze the intercalation kinetics with including the blocking effect by residual cations:

$$\dot{n} = \alpha(1 - n\beta),$$

where α, n, and β are the cation transfer rate, average cation

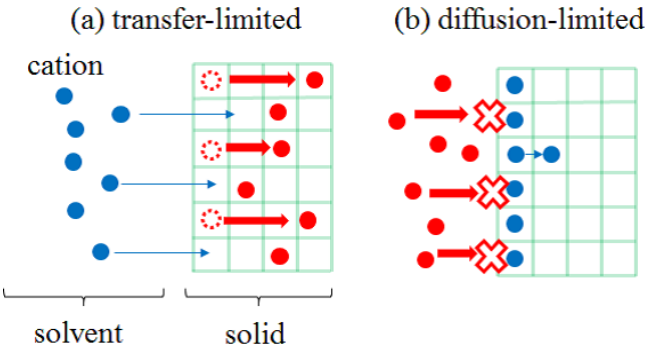

Fig. 3: Schematic illustrations of cation intercalation: (a) transfer-limited and (b) diffusion-limited cases.

density in solid, and residual coefficient, respectively. Note that n and α is normalized by number of the nanospaces of PBA, *i.e.*, two spaces per Ni. We assume that α is independent of time, because the cation capacity (= 0.2 μmol/cm^2) of the film is too low to seriously alter the electrolyte concentration around the interface. $n\beta$ is the density of the residual cation at the surface, which blocks the subsequent cation transfer from the solvent. We know that β is infinite at t = 0 and gradually decreases with t in a diffusion equation with semi-infinite boundary condition. Nevertheless, we treat β as a material parameter to obtain a perspective view for the cation diffusion effect on the intercalation kinetics. The cation intercalation stops at $n = 1/\beta$, because all the cation channels close. The equation at $\beta = 1$ describes the high-D limit, because the cation density at the surface is the same as the average (= n). The parameters, α and β, are determined by I_0 and τ through the relation:

$$I(t) \propto \dot{n} = \alpha \cdot \exp(-\alpha\beta t).$$

In Fig. 2(c) and (d), we plotted α and β against V_s - V_{ex}. Significantly, β in NNF67 is ~ 1 irrespective of the concentration and kind of the cation in soluvent. We note that β for the powder sample is ≈ 1 even though α is much lower than those in NNF67. These observations indicate that the fast cation intercalation is ascribed to the high-D value of nickel hexacyanoferrates. On the other hand, β (~ 50) in NCF88 is much higher than unity, indicating that the cation intercalation is limited by the slow cation diffusion.

In conclusion, we reported an ultrafast cation intercalation in a thin film of nickel hexacyanoferrate. We ascribed the fast intercalation to the fast cation diffusion in solid. We proposed a simple model to evaluate the residual cation effect, which is easily applicable to the other intercalation phenomena, *e.g.*, Li^+/Na^+ intercalation in aprotic solution (see Fig. S10).

This work was supported by the Mitsubishi foundation and also by the Grant-In-Aid (25620036) for Scientific Research from the Ministry of Education, Culture, Sports, Science and Technology. We are thankful to Ms. Nakazawa for her support in early stages of this investigation.

References

1 S. Kitagawa R. Kitaura, and S. Noro, Angew. Chem., Int. Ed., 2004, **43**, 2334.
2 S. Kaye and J. R. Long, J. Am, Chem. Soc., 2005, **127**, 6506.
3 K. Itaya, I. Uchida, V. D. Neff, Acc. Chem. Res., 1986, **19**, 162.
4 K. Itaya, T. Ataka, and S. Toshima, J. Am. Chem. Soc., 1982, **104**, 4767.
5 B. J. Feldman and O. R. Melroy, J. Electroanal. Chem., 1987, **234**, 213.
6 C. A. Lundgren and R. W. Murray, Inorg. Chem., 1988, **27**, 933.
7 C. Gabrielli, J. J. García-Jareño, M. Keddam, H. Perrot, and F. Vicente, J. Phys. Chem., 2002, **106**, 3182.
8 T. Shibata, F. Nakada, H. Kamioka and Y. Moritomo, J. Phys. Soc. Jpn., 2008, **77**, 104714.
9 F. Nakada, H. Kamioka, Y. Moritomo, J. E. Kim, and M. Takata, Phys. Rev. B, 2008, **77**, 224436.
10 K. Igarashi, F. Nakada and Y. Moritomo, Phys. Rev. B, 2008, **78**, 235106.
11 D. Ellis, E. Eckhoff, and V. D. Neff, J. Phys. Chem, 1081, **81**, 1225.
12 J. W. McCargar, V. D. Neff, J. Phys. Chem, 1988, **92**, 3698.
13 Y. Lu, L. Wang, J. Chung and J. B. Goodenough, Chem. Commun., 2012, **48**, 6544.
14 L. Wang, Y. Lu, J. Liu, M. Xu, J. Cheng, D. Zhang and J. B. Goodenough, J. B. Angew. Chem., 2013, **52**, 1964.
15 R. Y. Wang, C. D. Wessells, R. A. Huggins and Y. Cui, Nano Lett., 2013, **13**, 5748.
16 S. Yagi, M. Fukuda, R. Makiura, T. Ichitsubo, and E. Matsubara, J. Mater. Chem. A, 2013, **2**, 8041.
17 T. Matsuda and Y. Moritomo, Appl. Phys. Express, 2011, **4**, 047101.
18 T. Matsuda, M. Takachi and Y. Moritomo, Chem. Commun., 2013, **49**, 2750.
19 M. Takachi, T. Matsuda and Y. Moritomo, Appl. Phys. Express, 2013, **6**, 0425802.
20 Y. Mizuno, M. Okubo, E. Hosono, T. Kudo, H. Zhou, K. Ohishi, J. Phys. Chem. C, 2013, **117**, 10877.
21 M. Okubo, D. Asakura, Y. Mizuno, J.-D. Kim, T. Mizokawa, T. Kudo, I. Honma, J. Phys. Chem. Lett., 2010, **1**, 2063.
22 H. Lee, Y. Kim, J. Park, J. W. Choi, Chem. Commun., 2012, **48**, 8416. 8418.
23 D. Asakura, C. H. Li, Y. Mizuno, M. Okubo, H. Zhou, D. R. Talham, J. Am. Chem. Soc., 2013, **135**, 2793.
24 J. Luo, W. Cui, P. He, Y. Xia, Nat. Chem., 2010, **2**, 760.
25 P. Nie, L. Shen, H. Luo, B. Ding, G. Xu, J. Wang and X. Zhang, J. Mater. Chem., 2014, **2**, 5852.
26 P. Nie, L. Shen, H. Luo, H. Li, G. Xu, X. Zhang, Nanoscale, 2013, **5**, 11087.
27 Y. Mizuno, M. Okubo, E. Hosono, T. Kudo, H. Zhou, K. Ohishi, J. Phys. Chem. C, 2013, **117**, 10877.
28 M. Verdaguer, A. Bleuzen, V. Marvaud, J. Vaissermann, M. Seuleiman, C. Desplanches, A. Scuiller, C. Train, R. Garde, G. Gelly, C. Lomenech, I. Rosenman, P. Veillet, C. Cartier and F. Villain, Coord. Chem. Rev., 1999, **190-192**, 1023.
29 A. Ludi and H. U. Güdel, Struct. Bonding, 1973, **14**, 1.
30 M. Pyrasch, A. Toutianoush, W. Jin, J. Schnepf and B. Tieke, Chem. Mater., 2003, **15**, 245
31 W. Jin, A. Toutianoush, M. Pyrasch, J. Schnepf, H. Gottschalk, W. Rammensee, and B. Tieke, J. Phys. Chem. B, 2003, **107**, 12062.
32 A. J. Bard and L. R. Faulkner, "Electrochemical Methods" (John Willy & Sons, Inc. 1980).